Influence of Mn-site doping on charge and orbital ordering in $La_{1/3}Ca_{2/3}Mn_{1-y}M_yO_3$ manganites (M=Ni, Ga)

T. S. Orlova,[1,2] J. Y. Laval,[1] Ph. Monod,[1] P. Bassoul,[1] J. G. Noudem,[3] and E. V. Orlenko[4]
[1]*Laboratoire de Physique du Solide, CNRS ESPCI, 10 rue Vauquelin, 75231 Paris Cedex 05, France*
[2]*Ioffe Physical-Technical Institute of the Russian Academy of Sciences, 26 Polytekhnicheskaya, St. Petersburg 194021, Russia*
[3]*Laboratoire de Cristallographie et Sciences des Materiaux, ENSICAEN, 6 boulevard du Marechal Juin, 14050 Caen Cedex, France*
[4]*St. Petersburg State Polytechnical University, 29 Polytekhnicheskaya, St. Petersburg 194021, Russia*
(Received 22 July 2008; revised manuscript received 24 November 2008; published 6 April 2009)

The influence of Ni and Ga doping on orbital and charge ordering (CO) in $La_{1/3}Ca_{2/3}Mn_{1-y}M_yO_3$ (M: Ni, Ga, and $0 \leq y \leq 0.1$) has been investigated by combining magnetic and transport measurements with observation and analysis in transmission electron microscopy (TEM). Both types of doping cause a gradual decrease of T_{CO}—the temperature of the charge ordering transition—while the temperature dependences of the magnetization and electric resistivity remain typical of the CO state. In the undoped parent sample, direct observations by TEM reveal the extended commensurate striped superstructure with $\boldsymbol{q}$-vector $1/3\boldsymbol{a}^*$ over the whole temperature range <200 K. In Ni-doped samples, the long-range superstructure is kept but has an incommensurate character with reduced $\boldsymbol{q}$-vector by 18%–20% for Ni concentration $y=0.03$. The extent of the superstructure parameter modulation is in agreement with the resulting decrease in the concentration of Mn^{3+} ions due to their substitution by Ni^{2+}. Unlike doping by Ni, the incorporation of Ga on the Mn site completely suppresses the formation of the extended striped superstructure. Analysis of the obtained data allows us to conclude about the crucial role of the orbital-orbital (super)exchange interaction (rather than the Jahn-Teller interaction) in the stabilization of striped superstructure in the Mn-site-doped $La_{1/3}Ca_{2/3}MnO_3$ system.

DOI: 10.1103/PhysRevB.79.134407 PACS number(s): 75.47.Lx, 75.30.Et, 68.37.Lp, 64.70.Rh

I. INTRODUCTION

Numerous studies have been devoted to the manganites exhibiting colossal magnetoresistance (CMR) properties which are mainly based on double exchange phenomena[1,2] and Jahn-Teller effect (JT) of Mn^{3+} ion.[3] The phenomenon of colossal magnetoresistance[4] is generally agreed to be a result of the competition between crystal phases with different electronic, magnetic, and structural orders. The competition can be strong enough to cause a phase separation between metallic ferromagnetic (FM) and insulating charge-modulated [charge-ordered (CO)] states.[5,6]

Ferromagnetism and charge ordering are mutually exclusive phenomena in $R_{1-x}A_xMnO_3$ manganites where R is a trivalent rare-earth cation and A is a divalent cation. Ferromagnetism requires the delocalization of e_g electron from Mn^{3+} ion and its transfer along Mn^{3+}-O-Mn^{4+} network by double exchange interaction.[1] Charge ordering is realized by the localization of e_g electron and hole on Mn^{3+} and Mn^{4+} sites, respectively, and ordering of these ions in a particular pattern (Ref. 7) leading to antiferromagnetic (AFM) ordering at a temperature T_N.

The origin of charge- and orbital-ordered phase in the manganese perovskites is still the subject of debate.[8,9] Charge-orbital modulation has been traditionally considered as the ordering of Mn^{3+} and Mn^{4+} ions followed by ordering Jahn-Teller distortions of the $Mn^{3+}O_6$ octahedra; consequently, $d(z^2)(Mn^{3+})$ orbitals are oriented perpendicular to the c axis and form a series of ordered (zigzag) chains within the (a-b) basal plane.[7] The lattice distortions ordering can be perfectly detected in transmission electron microscopy (TEM). In $La_{1-x}Ca_xMnO_3$ (LCMO) system for special doping ($x=1/2$, 2/3 and 3/4), the superstructural modulation with the averaged wave vector $\boldsymbol{q}=(1-x)\boldsymbol{a}^*$ ($\boldsymbol{a}^*$ is the reciprocal-lattice vector) was observed by TEM.[10,11] However, according to some recent experimental findings (Refs. 12 and 13), the charge difference between two Mn sites is much less than 1. For example, two different Mn sites (one of which is distorted) were found in $Nd_{0.5}Sr_{0.5}MnO_3$ by using the resonant scattering of an intense synchrotron-generated x-ray beam. However, the charge difference between two configurations was only 0.16 electrons (Ref. 12) that is too far from $3d^3$ and $3d^4$ states accepted in the ionic model for Mn^{4+} and Mn^{3+}, respectively. As correctly noted in Ref. 9, the ionic picture is really only a starting point and it is necessary to take the oxygen $2p^6$ shell into account; moreover, the question on what drives the charge/orbital ordering: Jahn-Teller distortion versus orbital-orbital superexchange is still open.[14] Thus more experimental studies and theoretical considerations are needed to shed light on charge and orbital ordering phenomena. Modifying of Mn^{3+}-O-Mn^{4+} bonds, which are responsible for the interplay between ion, orbital, and spin orderings through the Mn site doping could be an efficient key in understanding the main factors affecting the charge-orbital ordering in the manganites.

Many papers have been devoted to the study of Mn site doping effects in $R_{1/2}A_{1/2}MnO_3$ manganites with $Mn^{3+}/Mn^{4+}=1$ ratio (see, for example, Refs. 15–20). Such doping by a small amount of certain element (M) can lead to drastic changes in the physical properties of $R_{1/2}A_{1/2}Mn_{1-y}M_yO_3$ manganites. For example, the insulator-metal transition was found in $Pr_{1/2}Ca_{1/2}Mn_{1-y}Cr_yO_3$ (Ref. 16) and $Nd_{1/2}Ca_{1/2}Mn_{1-y}Cr_yO_3$ (Ref. 21) compounds in a wide doping range ($0.02 \leq y \leq 0.07$). However, the mechanism of such drastic effects of Cr on charge-orbital ordering in these materials is still not understood. Manganites with a ratio

$Mn^{3+}/Mn^{4+}=1$ are often located on the phase diagram border between FM and AFM ground states and as a result are very sensitive to the small variation in the cation ratio or oxygen content. In addition, the presence of phase separation, which is typical for such "boundary" compounds, hinders the study of doping effect on charge-orbital ordering in pure CO case.

In electron rich $R_{1-x}A_xMnO_3$ ($x>0.5$) manganites, the effect of Mn site doping has not been studied systematically. Only few papers were devoted to such doping. For instance, the substitution of Mn sites by Cr, Co, Ni, and Ru in $Pr_{1-x}Ca_xMnO_3$ were studied for $x=0.6$ in Ref. 16. It was found that in this compound the insulator-metal transition was not induced by doping with Co or Ni, whereas doping by Cr and Ru caused such transition.

No systematic study of the influence of the Mn-site initial doping on striped charge-orbital ordering in $R_{1-x}A_xMnO_3$ ($x=2/3$, 3/4) compounds has been done, whereas such doping can lead to a better understanding of these phenomena.

We have studied the effect of doping through the substitution of Mn site by Ni and Ga, on charge and orbital ordering in the $La_{1/3}Ca_{2/3}MnO_3$ parent compound. This system was chosen for the following reasons. First, the ground state of this parent compound is located far from FM/AFM border in the phase diagram, hence small variations in the cation ratio or in oxygen content are not as critical as for the compound $La/Ca=Mn^{3+}/Mn^{4+}=1$. Second, in $La_{1/3}Ca_{2/3}MnO_3$ the phase separation is negligible.[22,23] FM fraction does not exceed 0.3% of the saturation value.[23] These facts allow us to study the effect of doping on CO phenomena in a purer case.

The effect of Fe doping on charge ordering in $La_{1/3}Ca_{2/3}Mn_{1-y}Fe_yO_3$ was studied in Ref. 23. It was found that T_{CO} is proportional to the concentration of Mn^{3+} ions and that Fe strongly modifies the superstructure inducing incommensurability. The $\boldsymbol{q}$ vector of a 5% Fe-doped sample is reduced by about 12%–15% compared to the undoped parent compound. Some defects responsible for incommensurability were revealed in the stripes ordering.

In the present work, the doping effects of diamagnetic Ga and magnetic Ni impurities on Mn sites in $La_{1/3}Ca_{2/3}MnO_3$ have been systematically studied by combining local fine compositional analysis [energy selective x-ray (EDX) *in situ* in scanning electron transmission microscope (STEM)] and structural determination in TEM [diffraction and high-resolution electron microscopy (HREM) images] with magnetic and transport measurements. The obtained data are compared with the results on Fe doping.[23] The experimental results allow us to conclude about the determining role of orbital-orbital superexchange interaction versus Jahn-Teller distortion interaction for the striped superstructure stabilizing in the Mn-site-doped $La_{1/3}Ca_{2/3}MnO_3$.

II. EXPERIMENTAL DETAILS AND SAMPLES CHARACTERIZATION

All the polycrystalline $La_{1/3}Ca_{2/3}Mn_{1-y}M_yO_3$ (M: Ni with $0\leq y\leq 0.1$ and Ga with $y=0.03$, 0.05) samples were prepared according to the same solid-state reaction similarly as was done in Ref. 23. Starting powders of La_2O_3, $CaCO_3$, MnO_2, and NiO (or Ga_2O_3, respectively) were mixed in stoichiometric proportions and heated twice in air at 900 °C–1200 °C for 24 h with intermediate grindings. Cold forming was performed under a uniaxial pressure of 30 MPa. The preformed pellets were conventionally sintered at 1300 °C during 24 h in air.

The prepared samples were characterized by powder x-ray diffraction (XRD) using a Philips automated x-ray diffractometer with Cu K_α radiation. In addition, *in situ* in STEM local (1–2 nm probe) compositional analysis was performed with a Princeton Gamma-Tech energy selective x-ray Si-Li analyzer attached to the STEM. Samples for electron microscopy were thinned by mechanical polishing followed by argon ion milling down to the electron transparency ($\leq$50 nm).

The electron diffraction (ED) versus temperature and lattice images were carried out at room temperature and at low temperature down to 91 K with a Jeol 2010 F transmission electron microscope operating at 200 kV and equipped with a field-emission gun [(FEG)-TEM] and a Gatan double tilt liquid N_2 sample holder (tilt $\pm 15°$ and $90\leq T\leq 300$ K). The images were processed with digital micrograph.

The resistance measurements were performed by the four-probe technique. The temperature dependence of the magnetization $M(T)$ in the temperature range 4.2–400 K was measured with a commercial quantum design superconducting quantum interference device (SQUID) magnetometer after cooling the samples from room temperature down to 4.2 K in zero-field [zero-field cooling (ZFC)] or in different dc magnetic fields H [field cooling (FC)].

Powder x-ray diffraction of all the studied compounds showed a single phase with perovskite structure (*Pbnm* space group) with $a\approx b\approx\sqrt{2}a_p$ and $c\approx 2a_p$ [where $a_p\sim 3.9$ Å is the lattice parameter of the simple perovskite structure (Ref. 10)]. No other phases or precipitates containing Ni or Ga were revealed. The estimation of lattice parameters from these data did not show any sizable variation with the dopant content. The precise correspondence between the obtained chemical composition and the nominal one was checked by local EDX analysis with a fine probe of 1–2 nm diameter *in situ* in STEM. For this purpose, we analyzed La:Ca:Mn:M ratio and distribution of the dopant in different positions within a grain and among about 15–20 different grains. The EDX results confirmed a good fit of compositions to the nominal ones and a very homogeneous distribution of Ga and Ni within grains. Variation in the dopant content in different points within a grain did not exceed 7% from the nominal values that is practically equal to the accuracy of the measurement. Both Ni and Ga did not segregate at grain boundaries and triple junctions. In Ni-doped samples, only few fine secondary phases of NiO were found in TEM.

The oxygen content was controlled by iodometric titration method described, for example, in Ref. 24. The analysis showed that the oxygen concentration was about the same in undoped and all doped compounds with low doping level ($y\leq 0.03$) and was close to the stoichiometric value 3.0; whereas for the higher concentration of dopants the oxygen content was somewhat lower (see Table I).

TABLE I. The results of iodometric titration.

Sample	Oxygen content(3-δ)
$La_{1/3}Ca_{2/3}MnO_{3-\delta}$	2.996
$La_{1/3}Ca_{2/3}Mn_{0.985}Ni_{0.015}O_{3-\delta}$	2.998
$La_{1/3}Ca_{2/3}Mn_{0.97}Ni_{0.03}O_{3-\delta}$	2.990
$La_{1/3}Ca_{2/3}Mn_{0.93}Ni_{0.07}O_{3-\delta}$	2.957
$La_{1/3}Ca_{2/3}Mn_{0.97}Ga_{0.03}O_{3-\delta}$	2.987
$La_{1/3}Ca_{2/3}Mn_{0.95}Ga_{0.05}O_{3-\delta}$	2.950

III. RESULTS

We first performed a comparative study of magnetization M as a function of temperature for $La_{1/3}Ca_{2/3}Mn_{1-y}M_yO_3$ (M: Ni with $0 \leq y \leq 0.1$ and Ga with $y=0.03$ and 0.05). The experimental curves measured at $H=1$ T are plotted in Fig. 1(a) for Ni-doped samples and in Fig. 1(b) for Ga-doped ones.

For $y=0$ sample, the $M(T)$ curve displays a peak at T_{CO} which is characteristic of charge-orbital ordering in LCMO and well described in the literature, for example, in Refs. 23 and 25. The transition temperature $T_{CO}=272$ K is close to

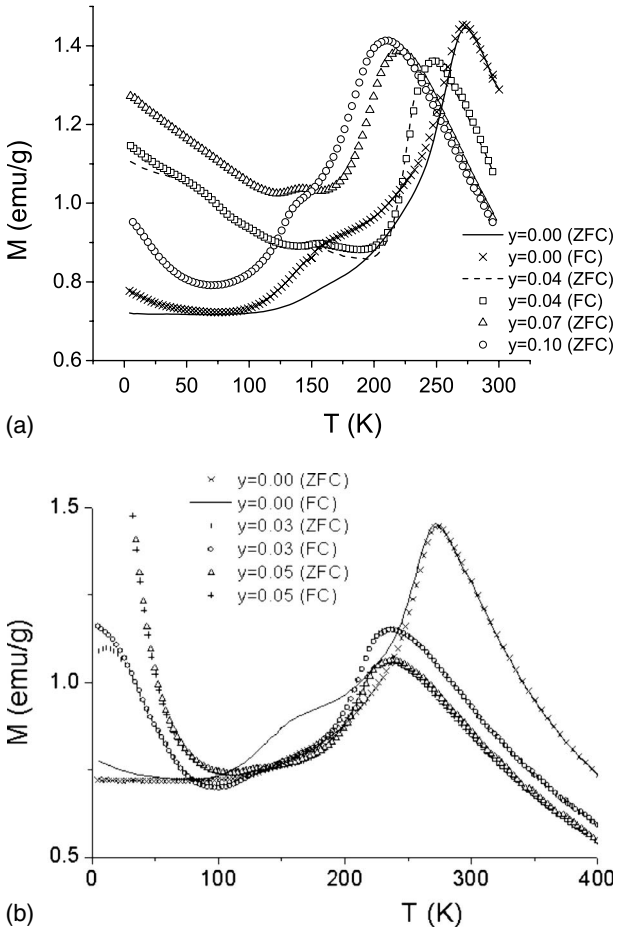

FIG. 1. Temperature dependences of ZFC and FC magnetizations for $La_{1/3}Ca_{2/3}Mn_{1-y}M_yO_3$ compounds with (a) M=Ni, (b) Ga, and $0 \leq y \leq 0.1$ in magnetic field $H=1$ T.

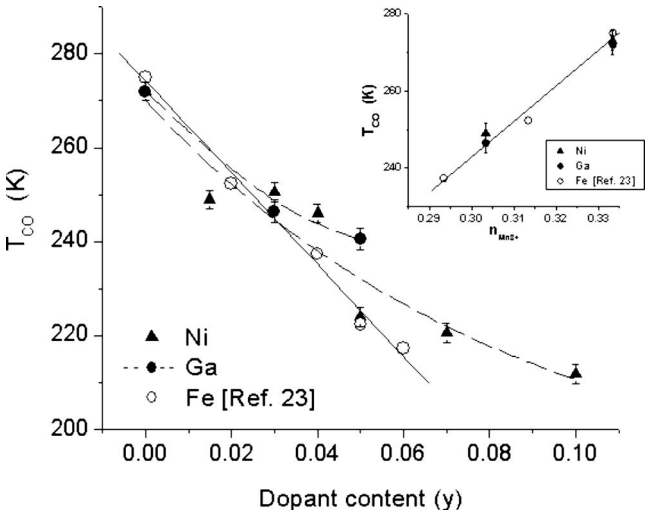

FIG. 2. Temperature T_{CO} of charge-ordering transition versus dopant concentration y for $La_{1/3}Ca_{2/3}Mn_{1-y}M_yO_3$ with M=Ni and Ga. For comparison, the case of Fe doping (Ref. 23) is also presented. Inset: T_{CO} versus the concentration $n_{Mn3+}=Mn^{3+}/(Mn^{3+}+Mn^{4+})$ of Mn^{3+} ions in the same compounds for low doping level ($y \leq 0.03$).

that commonly observed in high-temperature-synthesized $La_{1/3}Ca_{2/3}MnO_3$ polycrystals. The phase diagrams of $La_{1-x}Ca_xMnO_3$ system (Refs. 26 and 27) indicate that the ground state for $x=0.7$ compound is antiferromagnetic at low temperature with the Néel temperature $T_N \sim 170$ K.

Doping by Ni and Ga does not change the principal character of $M(T)$ curves but shifts T_{CO} substantially. The dependence of T_{CO} on dopant concentration y is shown in Fig. 2. For comparison, the case of Fe doping in $La_{1/3}Ca_{2/3}Mn_{1-y}Fe_yO_3$ from Ref. 23 is also presented. T_{CO} decreases gradually with the dopant content for both Ni and Ga impurities. It is noteworthy that for low doping level (for $y<0.03$, at least), the rates of T_{CO} decrease with dopant concentration y are comparable for Ga and Fe and somewhat lower than for Ni.

In Figs. 1(a) and 1(b) for comparison some magnetization-temperature dependences measured in an applied magnetic field $H=1$ T are shown for both measuring regimes: ZFC and FC. As seen, in the parent compound the difference between FC and ZFC magnetizations is small for $H=1$ T and doping by Ni or Ga does not increase it. This implies that neither dopant contributes to the FM component. In order to determine the ferromagnetic component, we measured the magnetization versus magnetic field H up to 5 T for the Ni-doped compounds and estimated the remanent magnetization at 5 K. A magnetic remanence $\Delta m < 0.01 \mu_B$/f.u. (Bohr magneton per formula unit) was found, which is comparable with Δm in the undoped sample (Ref. 23) and less than 0.3% of the idealized saturated magnetic moment. This suggests that Ni does not cause any substantial increase in FM component and it remains negligible.

We estimated the Curie-Weiss temperature θ from the $M(H)$ dependence in the temperature range $T > T_{CO}$ of paramagnetic behavior, where there is a good agreement with the Curie-Weiss law,

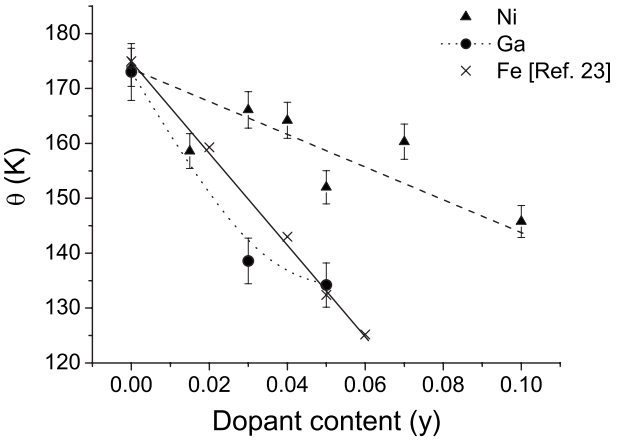

FIG. 3. Dependence of Weiss temperature θ on the dopant concentration for $La_{1/3}Ca_{2/3}Mn_{1-y}M_yO_3$ with M=Ni and Ga. For comparison, the case of Fe doping (Ref. 23) is also presented.

$$\chi = \frac{M}{H} = \frac{C^*}{T-\theta}. \quad (1)$$

In Eq. (1), $C^* = \frac{p_{\text{eff}}^2 \mu_B^2 N}{3k_B}$, p_{eff} is the effective Bohr magneton number per magnetic ion and θ is the Weiss temperature, and k_B is the Boltzmann constant. The estimated values of θ were plotted versus dopant concentration y as shown in Fig. 3. The $\theta(y)$ behavior for the Ni- and Ga-doped systems is compared with similar dependence obtained earlier (Ref. 23) when doping the same parent compound with Fe. The positive paramagnetic Curie-Weiss temperature θ indicates that ferromagnetic interactions are dominant in the temperature range of the paramagnetic behavior. Antiferromagnetic ordering at low temperatures is induced by the charge ordering which occurs at higher temperature T_{CO} than θ. θ gradually decreases when both Ni and Ga dopant content increases. Ga^{3+} is a diamagnetic impurity; hence the observed decrease in θ value could be mainly due to decreasing the contribution of FM exchange between Mn^{3+} and Mn^{4+} ions caused by the decrease in concentration of Mn^{3+} ions resulting from their substitution by Ga^{3+} ions. A stronger decrease could come from an AFM exchange between impurity ion and ⟨Mn⟩. Since the rate of θ decrease with Ni concentration is much lower compared with doping by diamagnetic Ga^{3+}, it seems that the resulting exchange between Ni and ⟨Mn⟩ ions is FM but weaker than FM exchange between Mn^{3+} and Mn^{4+} ions.

Figure 4 shows the temperature dependence of the resistivity $\rho(T)$ of Ni- and Ga-doped samples for some values of dopant concentration y (the curves corresponding to other studied compounds are omitted for the sake of clarity). The character of the $\rho(T)$ dependence does not change with both Ni and Ga dopings and remains typical for CO state at $T < T_{CO}$ for each compound. The samples remain essentially semiconducting over the entire temperature range 5–300 K and there is no insulator-metal (IM) transition when y value is increased for both types of dopants.

The influence of doping by Ni and Ga on charge ordering structure was investigated by the direct observation of ED patterns obtained from selected areas within grains and

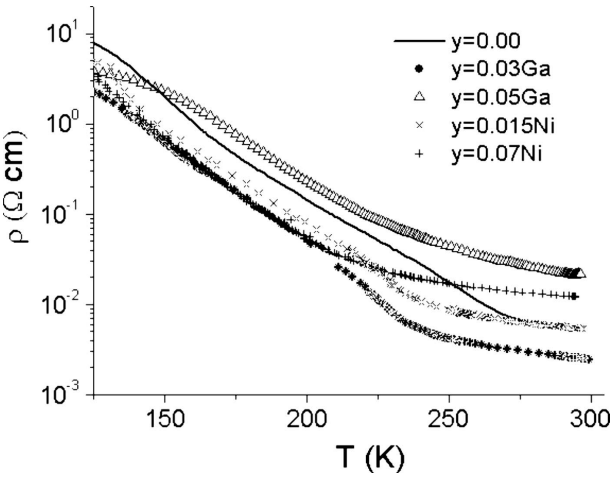

FIG. 4. Temperature dependence of resistivity of undoped $La_{1/3}Ca_{2/3}MnO_3$ and doped $La_{1/3}Ca_{2/3}Mn_{1-y}M_yO_3$ (M=Ni, Ga) compounds.

HREM imaging. The evolution of such ED patterns with temperature was investigated under temperature scanning from room temperature T_{room} down to 91–92 K with steps of 10°–20°. The appearance of a superstructure resulting from charge and orbital orderings is characterized by extra spots, in the reciprocal space, at position $\boldsymbol{q}$ from the main Bragg peaks.[21] In undoped sample, at 91 K, $\boldsymbol{q}$ was found to be equal to $1/3\boldsymbol{a}^*$ ($\boldsymbol{a}^*$ is the inverse lattice parameter). Formation of similar superstructure in the parent $La_{1/3}Ca_{2/3}MnO_3$ compound is known and reported, for example, in Refs. 10, 11, and 23. In Ref. 23 it was shown that in the case of fully oxygenated $La_{1/3}Ca_{2/3}MnO_3$, this superstructure has a commensurate character with $\boldsymbol{q}=1/3\ \boldsymbol{a}^*$ at $T<200$ K.

The [001] HREM image obtained at 91 K for 0.03 Ni-doped sample is shown in Fig. 5 together with the corresponding ED pattern. In this case, the sharp weaker satellite spots on the ED pattern can be indexed as $\boldsymbol{q}=(1/3\text{-}\varepsilon)\boldsymbol{a}^*$ with the parameter of incommensurability $\varepsilon \approx 0.060 \pm 0.005$, i.e., the superstructure in 0.03 Ni-doped sample is incommensurate. Our EDX analysis in TEM carried out exactly on the same selected area, where q value was determined, confirmed the good correspondence of the Ni content with the nominal one. It is important to point out that the observed superstructure extended over the whole crystal (grain) and was typical for all the studied grains (10–15 grains in each studied sample). In addition to the statistical general characterization of the dopant distribution in the studied samples (see Sec. II), Ni distribution was checked by local EDX (1–2 nm probe) *in situ* in STEM within the crystals (grains) where ED and HREM images were taken. Such analysis confirmed a homogeneously random distribution of the dopant and good correspondence of the real doping content to the nominal one. The estimation of the average value of $\boldsymbol{q}$ vector on several grains in 0.03 Ni sample gives $q = 0.275 \pm 0.010$ r.l.u. (reciprocal-lattice units) which is 17%–20% less than the q value in the parent compound.

The evolution of q value with temperature for 0.03 Ni-doped sample is shown in Fig. 6 in comparison with the undoped $La_{1/3}Ca_{2/3}MnO_3$. The temperature at which extra

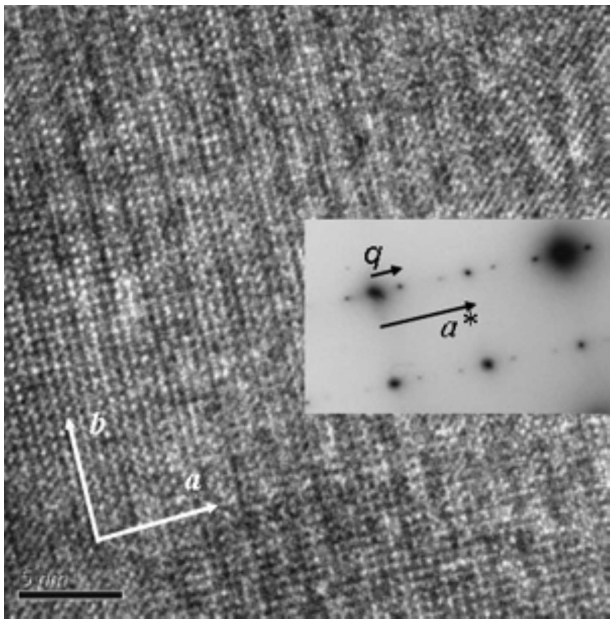

FIG. 5. HREM image of $La_{1/3}Ca_{2/3}Mn_{1-y}Ni_yO_3$ ($y=0.03$) with the electron-diffraction pattern from the same area recorded at $T=91$ K.

spots appear on ED patterns does correspond to T_{CO} determined from $M(T)$ measurements. The intensity of extra spots decreases when approaching T_{CO}. The extra spots give rise to streaking just before their disappearance at T_{CO}, as observed in the case of $La_{1/3}Ca_{2/3}Mn_{1-y}Fe_yO_3$ ($y=0.05$) samples in Ref. 23.

An estimation of the average periodicity of superstructure on the [001] HREM image (Fig. 5) yields approximately 20 Å which matches the obtained q value. Such an incommensurate superstructure could arise from some faults in $Mn^{3+}O_6$ and $Mn^{4+}O_6$ stripes arrangement and local variations in their periodicity. Although HREM images did reveal long-range extended superstructure, this superstructure does not show the sharp 1:2 periodicity of the stripes, which was observed in the undoped compound and was similar to that

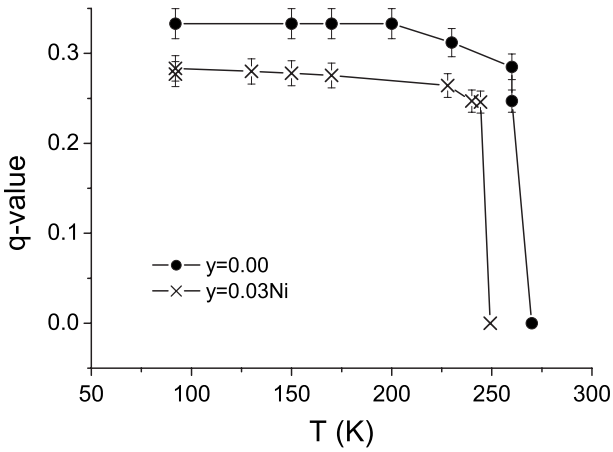

FIG. 6. q value in reciprocal-lattice units as a function of temperature for the undoped $La_{1/3}Ca_{2/3}MnO_3$ and doped $La_{1/3}Ca_{2/3}Mn_{1-y}Ni_yO_3$ ($y=0.03$) compounds.

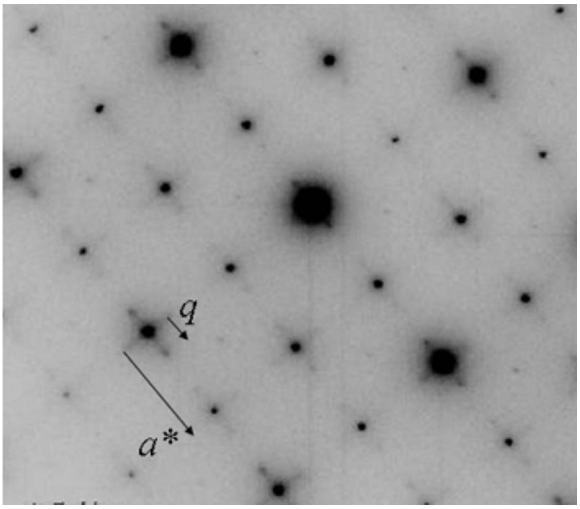

FIG. 7. [001] electron-diffraction pattern of $La_{1/3}Ca_{2/3}Mn_{1-y}Ni_yO_3$ ($y=0.07$) recorded at $T=91$ K. Extra spots and some streaking features are seen in positions $\boldsymbol{q}$ from main Bragg reflections.

shown in Ref. 23. Unfortunately, HREM images at low temperature were not sufficiently stable (due to mechanical vibrations) to allow for more details in the stripe arrangement in Ni-doped samples.

In order to check how an increase in the concentration of Ni will modify the CO/OO superstructure, we observed ED patterns for 0.07 Ni at 91 K and compared them with the ones for 0.03 Ni. An example of ED pattern at 91 K for 0.07 Ni is shown in Fig. 7. With the accuracy of our measurement, the average estimation of q parameter gives $q=0.270\pm0.010$ r.l.u. for 0.07 Ni which is comparable with $q=0.275\pm0.010$ r.l.u. for 0.03 Ni. For both compounds, combined EDX analysis confirmed that Ni concentration corresponds to the nominal one. We note that in 0.07 Ni sample, the extra spots are much weaker at 91 K in comparison with 0.03 Ni samples at the same temperature. Moreover, streaking is found around the Bragg spots as we observed in 0.03 Ni sample, only when approaching closely T_{CO}. Thus, the increase of Ni concentration up to $y=0.07$ affects the superstructure at 91 K in a similar way as approaching T_{CO} in the compound with $y=0.03$.

The TEM studies revealed striped superstructure only in the case of Ni-doped system, whereas on ED of Ga-doped samples extra spots typical for the CO/OO extended superstructure were not found at low temperatures down to 91 K. In Ga-doped samples, ED patterns at 91 K corresponded exactly to ED patterns at 300 K. However, the behavior of $M(T)$ and $\rho(T)$ of Ga-doped samples does not change in character compared with the undoped sample and remains typical for CO state. Similarly to the cases of Ni (this work) and Fe,[23] all the grains, where the ED patterns were taken, were checked by additional statistical local EDX analysis *in situ* in STEM. The analysis confirmed the uniform distribution of Ga in the grains and a good fit of Ga content to the nominal one.

IV. DISCUSSION AND CONCLUSIONS

Thus, for all doped compounds [Ni, Ga (this work), and Fe (Ref. 23)], the behavior of $M(T)$ and $\rho(T)$ does not

change in character as compared to the undoped sample and remains typical for CO state. However, the extended striped superstructure is kept only in the cases of Ni and Fe doping but is suppressed by Ga doping.

Although charge ordering is considered to be primarily caused by strong Coulomb interactions among the charge carriers of near neighbors,[28] such charge ordering is believed to be always accompanied by the cooperative JT orbital ordering (Refs. 7, 29, and 30), at least in half-doped manganites ($x=0.5$). As mentioned in Sec. I, in the manganites orbital ordering represents the ordering of $d(z^2)$ orbitals belonging to Mn^{3+} ions.

There exist in principle two different mechanisms of orbital ordering. First, it is the usual interaction of degenerate electrons with the crystal lattice,[31,32] which is usually considered as a source of Jahn-Teller effect. The formation of superstructures, including stripes, due to elastic interaction was considered in Refs. 33–35. The second mechanism is the electronic superexchange interaction,[36,37] which can give rise to both spin and orbital orderings, and which was quite successful in explaining the magnetic and orbital structures in a number of materials, for example, in cuprates.[36] In this mechanism, the structural transition (for example, ordering of distortions in manganites) is a secondary effect caused by electronic superexchange but not by direct Jahn-Teller interactions. Typically both of these mechanisms—the exchange interaction and the interaction via lattice—lead to the same orbital structures and the same ordering of the distortions in case of Jahn-Teller ions.[36] Apparently both these mechanisms are operational in real systems, and the relative importance of each is still an open problem, at least for the cases of manganites.[35] As it was correctly noted in Ref. 35, for manganites it is quite difficult to find the cases in which the outcomes of these two models would be qualitatively different. Doping on Mn sites in the $La_{1/3}Ca_{2/3}MnO_3$ compound which is located far from the FM/AFM border on the phase diagram seems to be efficient to distinguish between them.

As found in Ref. 23, doping by Fe^{3+} in $La_{1/3}Ca_{2/3}Mn_{1-y}Fe_yO_3$ did not cause the suppression of superstructure but only modified it by inducing some incommensurability. At the same time, the substitution of Mn^{3+} by Ga^{3+} in the similar amounts causes the suppression of orbital ordering, at least the long-range orbital ordering. In principle, a different ion on Mn site can also cause some "distortion" of these bonds due to difference in ionic size. But this is not the case of Fe^{3+} (0.645 Å) and Ga^{3+} (0.62 Å) since their ionic radii are comparable and relatively close to the ionic radius of Mn^{3+} (0.66 Å) or average ⟨Mn⟩ (0.58 Å) in the parent $La_{1/3}Ca_{2/3}MnO_3$ compound. Thus, no size effect is responsible for the difference between Fe and Ga effects on the superstructure stabilization.

Neither Fe^{3+} nor Ga^{3+} is a Jahn-Teller ion, hence they both are expected to influence similarly on a collective Jahn-Teller distortion interaction in the bulk lattice. However, their participation in the orbital-orbital superexchange will be different. Ga^{3+} and Fe^{3+} have different d-shell filling: active e_g electrons [$d(z^2)$ and $d(x^2\text{-}y^2)$] are present in Fe^{3+}, whereas Ga^{3+} is diamagnetic ion with totally filled d^{10}. Fe^{3+} with the active $d(z^2)$ electron on the place of Mn^{3+} in $Mn^{3+}O_6$ stripe can maintain orbital ordering through electronic (super)exchange, whereas Ga^{3+} with its totally filled d shell has no such possibility. Thus, the above argument allows us to conclude from our observations that in the doped $La_{1/3}Ca_{2/3}Mn_{1-y}M_yO_3$ compounds electronic (super)exchange is crucial for the stabilization of the striped superstructure.

The data obtained for Ni-doped compounds are in agreement with this conclusion too. As it will be shown below, the nickel ion in the considered manganite system has also active $d(z^2)$ electron; hence, it can contribute to stabilizing striped superstructure through orbital-orbital (super)exchange.

Although in Ref. 38 Ni was considered as trivalent in $La(MnNi)O_3$, the recent x-ray photoelectron spectra (XPS) and electron-paramagnetic-resonance (EPR) measurements in Ni-doped $(LaSr)MnO_3$ (Ref. 39) and $(LaCa)MnO_3$ (Ref. 40) both showed Ni ions in the divalent state with high-spin configuration. Moreover, in Ref. 41 it was shown by the x-ray absorption spectroscopy that the valence state shifts from Ni^{3+} in $LaNiO_3$ to Ni^{2+} in $LaNi_{0.5}Mn_{0.5}O_3$ and there is hybridization between Ni $3d$ and O $2p$ states. The latter, undoubtedly, also points out the high-spin configuration of Ni^{2+} state. The high-spin configuration of Ni^{2+} ion means $(6t_g2e_g)$ electronic state where $2e_g$ electrons: $3d_{x^2-y^2}$ and $3d_{z^2}$. The $\theta(y)$ dependences obtained in our work demonstrate much weaker decrease in temperature θ with the concentration of Ni compared with the case of diamagnetic Ga. This also implies indirectly that Ni in our compound possesses a magnetic moment.

Thus, let us consider two possible valence of Ni dopant for our compound. In the case of Ni^{2+} in the high-spin configuration, the active electrons, which can participate in the electron superexchange, will be nearly the same as in the case of Fe^{3+}, namely, $3d_{x^2-y^2}$ and $3d_{z^2}$. However, in the case of Ni^{2+} substitution for Mn^{3+}, the decrease in Mn^{3+} concentration will be equal to $2y$ when the oxygenation keeps the value 3.0. Then Mn^{3+} concentration in 0.03 Ni sample will be decreased by 0.06. The parameter of superstructure is determined by the relative concentration of ions participated in the formation of $Mn^{3+}O_6$ stripes, i.e., by Mn^{3+} ions and Ni^{2+} ions entering such stripes. It is important to recall that in manganite systems, no motion of manganese ions is required for the formation of stripes. Indeed, the stripes are formed by e_g electron transfer from Mn^{3+} to Mn^{4+}.[35] Of course, one should not take notations "3+" and "4+" for manganese ions too literally: as mentioned in Sec. I and pointed out in Ref. 35, actual degree of charge disproportion can be much less, e.g., $\sim(3.5\pm0.2)$. It seems that in the considered doped compounds, the formation of stripes occurs due to the transfer of e_g electrons belonging only to manganese ions. None of the considered impurities (Ni, Fe, and Ga) likely participates in the transfer of charges during the charge-orbital ordering because—regardless of the dopant type—the change in T_{CO} due to doping is proportional to the change in the relative concentration $n_{Mn3+}=Mn^{3+}/(Mn^{3+}+Mn^{4+})$ of Mn^{3+} ions, at least (see the inset to Fig. 2) for low doping level $y<0.03$ (where oxygenation is close to 3.0). Thus, formation of charge- and orbital-ordered structures occurs by means of manganese electron transfer and impurities met on the way of a forming stripe will or will not join in this orbital ordering in accordance with their d-shell structure. The last factor

seems to be critical for stabilizing or destabilizing long-range orbital ordering and, hence, stripe superstructure.

Roughly approximately 1/3 of all Ni ions can meet $Mn^{3+}O_6$ stripes because the doping ions are distributed regularly in the lattice and diffusion is absent in the considered temperature range 4.2–300 K. According to Chen *et al.*,[10] for manganites, corresponding to the formula of $La_{1-x}Ca_xMnO_3$, the q value was given by $q \sim (1-x)$. This means that in this system, the q value is proportional to the concentration of Mn^{3+} ions which formed $Mn^{3+}O_6$ stripes. For 0.03 Ni compound, such proportionality seems to be kept, since the estimation of q value, as $q=(1/3-2y+1/3y) \approx 0.283$ gives good agreement with the experimentally obtained value. Since doping by 3% Ni (Ni^{2+} ions) leads to the decrease in Mn^{3+} concentration even slightly higher than 5% Fe (Fe^{3+} ions) on Mn^{3+} sites,[23] it is clear why 3% Ni doping caused even a larger decrease in q value than 5% Fe in the same parent compound.[23] The higher doping level (0.07Ni) resulted in some oxygen deficiency (see Table I); the latter causes some additional change in ratio $Mn^{3+}:Mn^{4+}$ and formation of oxygen vacancies in the perovskite lattice. This seems to explain the fact why 7% of Ni did not practically cause the difference in q value as compared with 3% Ni and also the appearance of some imperfects in the ED pattern as the streaking. Deviation of $Mn^{3+}:Mn^{4+}$ ratio from 1:2 results in incommensurability of superstructure in the Ni-doped samples through the formation of some defects in their arrangement as it was observed for Fe-doped compound in Ref. 23.

But to be on the safe side, let us consider the case if Ni enter as Ni^{3+} ion. According to Ref. 42, the trivalent nickel in $LaNiO_3$ does not follow Hund's first rule; it is in a low-spin state, $3d^7: t_{2g}^6, e_g^1$, with $S=1/2$. Then both Ni^{3+} and Mn^{3+} have similar active e_g electron $[d(z^2)]$ which can participate in the orbital-orbital superexchange and maintain the stripe formation. Similarly to Ni^{2+} considered above, not every Ni^{3+} ion will participate in building of $Mn^{3+}O_6$ stripes (diffusion processes of transition elements are not active in the considered temperature range); the resulting superstructure would not be commensurate, too. However, in the case of Ni^{3+} substitution for Mn^{3+}, the value of incommensurability would be much less than the experimentally observed one in 0.03 Ni sample because Ni^{3+} substitution for Mn^{3+} causes a decrease in Mn^{3+} concentration only by y value. Then in the studied Ni-doped $La_{1/3}Ca_{2/3}Mn_{1-y}Ni_yO_3$ samples, Ni ion is most likely divalent.

Ga^{3+} ion replacing Mn^{3+} in the chain has a $3d^{10}$-filled electronic structure. That means that there is no opportunity for the realization of superexchange and simple interatomic electron exchange. Such a doping is diamagnetic. Substitution of Mn^{3+} by diamagnetic Ga^{3+} cannot contribute to orbital ordering, leading thereby to some orbital disordering which can appear as frustration of e_g orbital of neighboring Mn^{3+} ions in $Mn^{3+}O_6$ stripe. Such disordering can cause a complete break in the long-range-striped orbital ordering or lead to the formation of very small nanosized domains with the OO. Actually, 3% of Ga on Mn sites corresponds to the average Ga-Ga separation equal to only ~3.2 l.u. (in lattice units, here 1 l.u. ≈ 3.9 Å). Thus we suggest that in Ga-doped samples, CO exists but Mn^{3+} e_g orbitals around Ga^{3+} ions are fluctuating, creating subtle variations in the Mn-O-bond lengths. Since ED is more sensitive to local lattice distortions induced by the orbital ordering rather than to charge ordering itself,[19] most probably because of this reason we cannot observe the striped superstructure (without orbital ordering or with tiny domains with OO) by TEM. Thus, the striped orbital ordering and charge ordering seem to be decoupled in Ga-doped samples. Such a decoupling of orbital ordering and charge ordering transitions was found experimentally in $Pr_{1/2}Ca_{1/2}Mn_{1-x}Cr_xO_3$ with $x=0.05$.[19] Thus, neither of the two magnetic dopants Ni (this work) and Fe (Ref. 23), in $La_{1/3}Ca_{2/3}Mn_{1-y}M_yO_3$ suppresses the striped superstructure, inducing only incommensurability, whereas diamagnetic Ga^{3+} does suppress it.

Depending on d-shell structure, some impurities (Fe and Ni) can maintain striped CO/OO superstructure through the orbital-orbital exchange or superexchange, modifying only the superstructure parameter, whereas some other impurities (Ga, for example) destabilize it. It is noteworthy that impurities with different d-shell structure in comparison with manganese ions probably can also disturb locally the magnetic order in manganese chains even if they participate in orbital-orbital (super)exchange through active electrons on their d shell. In turn, such local change in magnetic ordering probably can affect the long-range CO/OO superstructure. There is a need for special theoretical analysis on the influence of d-shell structure of doping impurities on the resulting orbital and magnetic ordering in $\langle M \rangle$-O-$\langle$Mn$\rangle$ chains through (super)exchange.

In conclusion, our experimental results have shown that the substitution of Mn site by magnetic Ni (or by Fe in Ref. 23) and diamagnetic Ga leads to a gradual decrease of T_{CO} with the dopant concentration y; the T_{CO} decrease being proportional to the change in the Mn^{3+} ion concentration caused by the doping. The character of magnetization and semiconducting behavior of resistivity at low temperatures remains typical for CO state for both types of doping. The direct observation in TEM in the temperature range 91–300 K has shown that the transition at T_{CO} is accompanied by the formation of extended incommensurate superstructure in Ni-doped series with a strongly decreased q vector (by 17%–20% in 3% Ni-doped sample) compared with the parent compound. Similar to Fe doping,[23] the extent of the q-parameter modulation is proportional to the decrease in the concentration of Mn^{3+} ions in the case of their substitution by Ni^{2+} ions. The latter along with the literature data[39–41] testifies that Ni enters $La_{1/3}Ca_{2/3}MnO_3$ manganite mostly as divalent. In Ga-doped samples, no features of low-temperature long-range superstructure were apparent by electron diffraction in TEM. Our microscopy data combined with magnetization and resistivity studies suggest that in $La_{1/3}Ca_{2/3}MnO_3$, the doping by diamagnetic impurity Ga^{3+} with d^{10} orbital results in the suppression of long-range-striped superstructure. Since both of the studied impurity ions Ga^{3+} and Ni^{2+} (in the orthogonal symmetry), as well as Fe^{3+} (Ref. 23), are non-Jahn-Teller ions, the obtained data allow us to conclude that the orbital-orbital (super)exchange interaction (rather than the Jahn-Teller interaction) plays a crucial role in the stabilization of the striped superstructure in the Mn-site-doped $La_{1/3}Ca_{2/3}MnO_3$ compounds.

ACKNOWLEDGMENTS

T.S.O. is very grateful to ESPCI de Paris for the invitation and support of her as a visiting researcher. The authors thank Yu. P. Stepanov for carrying out of the iodometric titration analysis of the oxygen content in the studied samples and to V. S. Vikhnin and to G. G. Zegrya for fruitful discussions.

[1] C. Zener, Phys. Rev. **81**, 440 (1951).
[2] P. G. de Gennes, Phys. Rev. **118**, 141 (1960).
[3] A. J. Millis, P. B. Littlewood, and B. I. Shraiman, Phys. Rev. Lett. **74**, 5144 (1995).
[4] *Colossal Magnetoresistance Oxides*, edited by Y. Tokura (Gordon and Breach, New York, 2000).
[5] E. Dagotto, H. Hotta, and A. Moreo, Phys. Rep. **344**, 1 (2001).
[6] E. L. Nagaev, *Colossal Magnetoresistance and Phase Separation in Magnetic Semiconductors* (Imperial College, London, 2002).
[7] J. B. Goodenough, Phys. Rev. **100**, 564 (1955).
[8] G. C. Milward, M. J. Calderon, and P. B. Littlewood, Nature (London) **433**, 607 (2005).
[9] M. Coey, Nature (London) **430**, 155 (2004).
[10] C. H. Chen, S.-W. Cheong, and H. Y. Hwang, J. Appl. Phys. **81**, 4326 (1997).
[11] S. Mori, C. H. Chen, and S.-W. Cheong, Nature (London) **392**, 473 (1998).
[12] J. Herrero-Martin, J. Garcia, G. Subias, J. Blasco, and M. Concepcion Sánchez, Phys. Rev. B **70**, 024408 (2004).
[13] J. Garcia, M. Concepcion Sánchez, J. Blasco, G. Subias, and M. Grazia Proietti, J. Phys.: Condens. Matter **13**, 3243 (2001).
[14] U. Staub, V. Scagnoli, A. M. Mulders, M. Janousch, Z. Honda, and J. M. Tonnerre, Europhys. Lett. **76**, 926 (2006).
[15] C. Martin, A. Maignan, and B. Raveau, J. Mater. Chem. **6**, 1245 (1996).
[16] B. Raveau, C. Martin, A. Maignon, M. Hervieu, and R. Mahendiran, Physica C **341-348**, 711 (2000).
[17] S. Hebert, A. Naignan, V. Hardy, C. Martin, M. Hervieu, and B. Raveau, Solid State Commun. **122**, 335 (2002).
[18] B. Raveau, A. Maignan, and C. Martin, J. Solid State Chem. **130**, 162 (1997).
[19] R. Mahendiran, M. Hervieu, A. Maignan, C. Martin, and B. Raveau, Solid State Commun. **114**, 429 (2000).
[20] G. Van Tendeloo, O. I. Lebedev, M. Hervieu, and B. Raveau, Rep. Prog. Phys. **67**, 1315 (2004).
[21] W. Schuddinck, G. Van Tendeloo, A. Barnabe, M. Hervieu, and B. Raveau, J. Solid State Chem. **148**, 333 (1999).
[22] Y. Jo, J.-G. Park, C. S. Hong, N. H. Hur, and H. C. Ri, Phys. Rev. B **63**, 172413 (2001).
[23] T. S. Orlova, J. Y. Laval, P. Monod, J. G. Noudem, V. S. Zahvalinskii, V. S. Vikhnin, and Yu. P. Stepanov, J. Phys.: Condens. Matter **18**, 6729 (2006).
[24] W. M. Chen, J. Chen, and X. Jin, Physica C **276**, 132 (1997).
[25] M. T. Fernandez-Diaz, J. L. Martinez, J. M. Alonso, and E. Herrero, Phys. Rev. B **59**, 1277 (1999).
[26] P. Schiffer, A. P. Ramirez, W. Bao, and S.-W. Cheong, Phys. Rev. Lett. **75**, 3336 (1995).
[27] M. R. Ibarra, J. M. De Teresa, J. Blasco, P. A. Algarabel, C. Marquina, J. Garcia, J. Stankiewicz, and C. Ritter, Phys. Rev. B **56**, 8252 (1997).
[28] S. K. Mishra, S. Rahul Pandit, and S. Satpathy, J. Phys.: Condens. Matter **11**, 8561 (1999).
[29] M. Tokunaga, N. Miura, Y. Tomioka, and Y. Tokura, Phys. Rev. B **57**, 5259 (1998).
[30] Z. Jirak, S. Krupicka, Z. Simsa, M. Dlouham, and S. Vratislav, J. Magn. Magn. Mater. **53**, 153 (1985).
[31] M. D. Kaplan and B. G. Vekhter, *Cooperative Phenomena in Jahn-Teller Crystals* (Plenum, New York, 1995).
[32] R. Englman, *The Jahn-Teller Effect in Molecules and Crystals* (Wiley-Interscience, New York, 1972).
[33] D. I. Khomskii and K. I. Kugel, Europhys. Lett. **55**, 208 (2001).
[34] D. I. Khomskii, Int. J. Mod. Phys. B **15**, 2665 (2001).
[35] D. I. Khomskii and K. I. Kugel, Phys. Rev. B **67**, 134401 (2003).
[36] K. I. Kugel and D. I. Khomskii, Usp. Fiz. Nauk **136**, 621 (1982) [Sov. Phys. Usp. **25**, 231 (1982)].
[37] K. I. Kugel and D. I. Khomskii, Zh. Eksp. Teor. Fiz. **64**, 1429 (1993) [Sov. Phys. JETP **37**, 725 (1973)].
[38] J. B. Goodenough, Phys. Rev. **124**, 373 (1961).
[39] X. Chen, Z. H. Wang, J. W. Cai, B. G. Shen, and W. S. Zhan, J. Appl. Phys. **86**, 4534 (1999).
[40] M. Rubinstein, D. J. Gillespie, J. E. Snyder, and T. M. Tritt, Phys. Rev. B **56**, 5412 (1997).
[41] M. C. Sanchez, J. Garcia, J. Blasco, G. Subias, and J. Perez-Cacho, Phys. Rev. B **65**, 144409 (2002).
[42] J. M. D. Coey, M. Viret, and S. von Molnar, Adv. Phys. **48**, 167 (1999).